Journal of Advanced Zoology

ISSN: 0253-7214

Volume ***45*** *Issue* ***2 Year 2024*** *Page* ***242:260***

Computational Approach To Evaluate The Potential Of Some Phytocompounds Of *Flacourtia Jangomas* Against Udp-Glf Enzyme Of *Mycobacterium Tuberculosis* (*Mtb*)

Sabina Begum Choudhury[1], Monjur Ahmed Laskar[2], Abhishek Chowdhury[2], Anupam Das Talukdar[1,2], Manabendra Dutta Choudhury[1,2,*]

[1]Department of Life Science and Bioinformatics, Assam University, Silchar, Assam 788011, India
[2]Bioinformatics and Computational Biology Centre, Assam University, Silchar, Assam 788011, India

****Corresponding Author**: Manabendra Dutta Choudhury*
Email address: drmdc@bioinfoaus.ac.in, Phone no. 9435173637

Article History

Received-05/12/2023
Revised-27/12/2023
Accepted-18/01/2024

Abstract

The ongoing usage of natural products since time immemorial has resulted in several beneficial medications derived from plant sources. Flavonoids are well known for their anti-bacterial role against a wide range of micro-organisms. Among them *Mycobacterium tuberculosis* (*Mtb*) is the bacterial agent, which is known to cause tuberculosis disease. Tuberculosis is considered as a worldwide health issue causing a wide range of morbidity and mortality every year. Due to the many challenges faced by the current treatment regimen, there is a need for new anti-tuberculosis drugs that have safety benefits. A vast range of natural compounds from different plant varieties were reported to be effective against *M.tuberculosis* in experimental conditions. In the current study, we have taken into consideration *Mtb*'s UDP-glf enzyme keeping in view the complexity of *Mtb* cell wall. As ligands, natural compounds obtained from the *Flacourtia jangomas* were used. This work mainly focuses on *in silico* methods and tools comprising molecular docking, QSAR, ADME/Tox profiling and molecular dynamics simulation of the suitable compound. The study indicated that among all the phytocompounds studied; mainly quercetin shows effective and better results compared to others which is supported by other findings too. *In vitro* and *in vivo* study with quercetin in relation to *Mtb* UDP-glf may provide forth insight for its applicability in controlling tuberculosis.

1. INTRODUCTION:

The issue of antibiotic resistance has become increasingly worrisome almost everywhere in the world over the past several years. This had appeared as one of the most pressing human health concern all over the globe (Liebenberg D et al; 2022).*Mycobacterium tuberculosis* (*Mtb*), a pathogenic bacteria and the main causative organism for causing tuberculosis (TB) disease, remains as the second leading infectious killer worldwide. In 2020, the disease killed 1.5 million instances and impacted 9.9 million people; in 2021, 10.6 million cases of tuberculosis were reported globally, and 1.6 million deaths were attributed to the disease (Chawla et al; 2022, Dean S. et al; 2022, WHO report 2022). As per the most recent WHO study, 10.6 million individuals were predicted to have contracted TB in 2022, of which 5.8 million were male, 3.5 million were female, and 1.3 million were small children. Additionally, 1.3 million people died from tuberculosis in 2022 (Global WHO

study, 2023). The common public has been seriously threatened by the rise of drug resistance (MDR-TB and XDR-TB), which also presents a significant obstacle to tuberculosis treatment (Adeniji et al., 2018). Despite being a disease that can be controlled, prevented, and cured, tuberculosis still remains as a serious community health concern in different parts of the world because of numerous flaws and failures. Thus, more research into alternative pathways and novel concepts for the worldwide eradication of this deadly disease should be considered (Cobelens et al., 2022).

The complexity of cell wall in*Mycobacterium tuberculosis* marks a distinguishing feature which are lacking in other prokaryotes (Alderwick et al; 2015). The structure of cell wall consists of three distinct layers- Peptidoglycan, arabinogalactan and mycolic acids. The mycolyl-arabinogalactan-peptidoglycan (mAGP) complex is crucial for promoting cell proliferation, pathogenicity, and acting as an antibiotic barrier (Abrahams K. et al. 2018 and Alderwick J et al. 2015). The peptidoglycan present in the cell wall of bacteria is necessary for the cell to survive, and the elements that comprise the bacterial cell wall's basic structure are crucial for pathogenicity and survival in addition to acting as permeability barriers that shield the cell from hydrophilic substances. These factors collectively make the cell wall components an important as well as attractive drug target (Maitra et al; 2019), (Abrahams K et al, 2018). Targeting the cell wall of the mycobacterial organism can be one of the methods for treating tuberculosis. The first-line TB medications - Ethambutol (EMB) and Isoniazid (INH) block important enzymes needed to make arabinogalactan and mycolic acids. Various researchers have found a large number of novel drug families that target essential proteins involved in the construction of the structural parts of the cell wall (Amado et al; 2022).

One of them is UDP-galactopyranose mutase (UGM), an enzyme containing flavin and an important enzyme in the mycobacterial cell wall biosynthesis and it can be considered as a potential target for the management of tuberculosis (Shi Y. et al; 2016, Van et al; 2015). It is encoded by the gene glf that catalyses the interconversion of UDP-galactopyranose (UDP-Galp) into UDP- galactofuranose (UDP-Galf) through a 2-keto intermediate, which is an important component in *Mycobacterium tuberculosis* for its cell construction (Weston et al; 1998, Soltero-Higgin et al; 2004, Van et al; 2015). Mycobacterial galactofuran production is crucial for mycobacterial survival because it links the cell wall layers of peptidoglycan and mycolic acid (Weston et al., 1998).

Research indicates that natural compounds are gradually being utilized as pharmacological leads, primarily to address antimicrobial resistance (Atanasov et al., 2021). The coffee plum, or *Flacourtia jangomas* (Lour.) Raeusch, is a small deciduos tree with a variety of therapeutic uses was used in this study (Mishra T et al; 2020). According to a number of studies and sources of information, *F. jangomas* include a wide range of different chemicals, including steroids, phenols, alkaloids, glycosides, tannins, flavonoids, and many more (Mishra T. et al., 2020, Pai A. and Shenoy K.C., 2020). The antimicrobial activity of the plant, *Flacourtia jangomas* have been reported by several researchers against a variety of pathogenic and non-pathogenic bacteria (Sasi et al., 2018, Kashyap et al., 2017, George et al., 2017, Shukla et al., 2015, Mishra T et al., 2020).

Therefore, in the present work an *in silico* study was taken up to analyse the phytocompounds from *Flacourtia jangomas* plant against *Mtb* protein keeping in view the extensive demand of computational methods for new drug discovery process. Molecular docking approach along with QSAR studies helps to determine the binding compatibility between the molecules and the target (ligand-receptor interaction) and correlate the Ic50 values with the molecular properties and bioactivity (Rosell-Hidalgo et al; 2021).

2. METHODOLOGY:

2.1 The receptors:

The validated three-dimensional structure of UDP-galactopyranose mutase having PDB ID: 4RPG (PDB DOI: https://doi.org/10.2210/pdb4RPG/pdb) was taken from the RCSB Protein Databank in .pdb format (www.rcsb.org/pdb). X-ray diffraction method having resolution 2.40 Å was used to to determine the crystal structure. The source organism, resolution, availability of ligand-bounded for active site reference, and active site residues were taken into consideration while choosing the structure. By creating a Ramachandran plot, the PROCHECK module, which is accessible on the PDBSum server has also been employed to assess the stereochemical quality of the structure.

2.2 The ligands:
Based on the literature survey, 16 (sixteen) compounds have been found to have isolated from the plant *Flacourtia jangomas* (Sasi et al; 2018, Saikia et al; 2016). The known inhibitor was also selected based on literature review. The National Center for Biotechnology Information's (NCBI) PubChem database provided the structures of these phytochemicals (http://pubchem.ncbi.nlm.nih.gov). We used Open Babel 3.1.1 to convert the .sdf files to .mol format. Finally the structure of these compounds was then drawn using ACD Free ChemSketch.

2.3 Molecular docking:
The molecular docking study was carried out with the help of the licensed version of BioSolveIT (LeadIT) FlexX 2.1.3. This is done to understand and visualize the interactions between a receptor and its ligand.With the aid of this program, the water molecules were removed from the workspace and the target's active site was initially determined by taking into account the amino acid residues.The receptor UDP-glf was then docked with the sixteen compounds each and also with its respective control. FlexX mostly makes use of an incremental building algorithm that takes into account the physical and chemical characteristics and changeable flexibility of compounds when placing them into the active site of the rigid target protein (Rarey et al., 1996). Several docking parameters such as bonded residues and scores which represent the energy values in Kcal/mol were calculated from the results.

2.4 QSAR Analysis:
QSAR, which compares a substance's physicochemical properties to those of compounds with experimental IC50 values, is now a tremendously important strategy in drug discovery research (Winkler, 2001; Mishra and Singh, 2015). Utilizing the whole list of known receptor inhibitors from the BindingDB database, the QSAR analysis was conducted. The QSAR descriptors for each molecule, such as the molecular weight, molecular volume, surface tension, density, logP, hydrogen bond acceptor and hydrogen bond donor, were produced using the ACD ChemSketch program. The regression equation was created using the free ligand activity prediction tool EasyQSAR. The F statistics was used to evaluate the correlation's significance and the equation's creation. A multiple regression plot was made for the QSAR model.

2.5 Prediction of ADME/Tox profile and drug-likeness:
A substance to be classified as an active drug, it must make it to its intended target in the body in the appropriate concentration and stay there in a bioactive state until the expected biological events take place. The best compound’s pharmacokinetics, drug similarity, and medicinal chemistry characteristics have been determined using the publicly available online Swiss ADME web tool (server) of the Swiss Institute of Bioinformatics (Daina et al., 2017). The bioavailability and brain toxicity of compounds under research are largely determined by pharmacokinetic factors such as gastrointestinal absorption and brain access. The Brain Or IntestinaL Estimate D permeation method (BOILED-Egg) is a graphical output method in Swiss ADME (Daina & Zoete, 2016) that uses the polarity (Topological Polar Surface Area, or TPSA) and lipophilicity (n-octanol/water partition coefficient, or WLOGP) of small molecules to predict their brain penetration and passive gastrointestinal absorption. All these parameters were calculated using the ADME tool. Also with the help of Molsoft L.L.C. online tool, a graph was plotted to show the drug nature of the compounds.
In addition, Molinspiration Cheminformatics, online software was also involved to obtain different parameters like MiLogP, TPSA, and other physico-chemical properties. While the TPSA parameter is a very helpful indicator of the drug transport capabilities, for checking good permeability across the cell membrane, the MiLogP parameter is being used. By evaluating the activity score against GPCR ligands, nuclear receptor ligands, protease inhibitors, kinase inhibitors, ion channel modulators, and enzyme inhibitors, this web-based tool also predicts the bioactivity of the substances (Kulkarni et al; 2021, Mohan et al; 2017).
Protox-II (https://tox-new.charite.de/protox_II/) (Banerjee et al., 2018) was utilized for toxicity study. It employs machine learning, pharmacophore fragment propensities, and chemical similarity to predict the toxicities of small compounds. The prediction of different toxicity endpoints, including hepatotoxicity, immunotoxicity, carcinogenicity, cytotoxicity. mutagenicity, unfavorable outcomes (Tox21) pathways, and toxicity target, is based on a total of 33 models.

2.6 Molecular dynamics simulation analysis:
To study and have a clear understanding about the protein’s structural stability, its atomic behavior and conformational changes, molecular dynamics (MD) simulation is the preferred method (Ahmad I et al.,

2023). The MD simulations experiments used in this article were conducted with the Desmond 2020.1 from Schrödinger, LLC. An independent simulation run at 37 °C was conducted. In this system (Jorgensen et al., 1983), an explicit solvent model with SPC water molecules and the OPLS-2005 force field (Bowers et al., 2006; Chow et al., 2008, Shivakumar et al., 2010) were utilized in a period boundary salvation box with dimensions of 10 Å x 10 Å x 10 Å. The 0.15 M charge was neutralized by the addition of Na+ ions. The system was supplemented with NaCl solutions to replicate the physiological milieu.The system was first retrained over the protein ligand complexes using an NVT ensemble for 10 ns. After the preceding phase, an NPT ensemble was used for a brief 12-ns run of equilibration and minimization. The Nose-Hoover chain coupling approach (Martyna et al., 1994) was used to set up the NPT ensemble. The simulations were conducted with a constant pressure of 1 bar, a relaxation time of 1.0ps, and a temperature variation. A 2fs time step was employed. The pressure was controlled using the barostat method and the Martyna-Tuckerman-Klein chain coupling system, with relaxation duration of two ps, (Martyna et al., 1992). The particle mesh Ewald approach was employed for the calculation of long range electrostatic interactions (Toukmaji et al., 1996), with a fixed radius of 9Å for the coulomb interactions. At a time step of 2fs, for each trajectory the bonded forces were computed using the RESPA integrator. The final production run lasted for one hundred nanoseconds each. To keep track if the MD simulations are stable or not, the following metrics were computed: solvent accessible surface area (SASA), radius of gyration (Rg), root mean square fluctuation (RMSF), and root means square deviation (RMSD).

Binding free energy analysis

The generalized Born surface area (MM-GBSA) method in combination with molecular mechanics was used to calculate the ligand-protein complexes' binding free energies. With the use of Python script thermal mmgbsa.py in the simulation trajectory for the last 50 frames with a 1-step sample size, the Prime MM-GBSA binding free energy was determined. By adding together several energy modules such as covalent, hydrogen bond, columbic, van der Waals, lipophilic, solvation of protein, and ligand, self-contact, the binding free energy of Prime MM-GBSA (kcal/mol) was calculated using the additivity principle. The equation forΔG_{bind} is calculated by the following equation:

$$\Delta G_{bind} = \Delta G_{MM} + \Delta G_{Solv} - \Delta G_{SA}$$

Where

- ΔG_{bind} designates the free energy of bonding,
- ΔG_{MM} designates difference between the free energies of ligand-protein complexes and the total energies of protein and ligand in isolated form,
- ΔG_{Solv} designates difference in the GSA solvation energies of the ligand-receptor complex and the sum of the solvation energies of the receptor and the ligand in the unbound state,
- ΔG_{SA} designates the difference in the surface area energies for the protein and the ligand.

3. RESULTS:

3.1 Receptor and ligands:

Receptor:
Name of the receptor (molecule): UDP-galactopyranose mutase (UGM)
PDB ID: 4RPG
Classification: Isomerase
Organism: *Mycobacterium tuberculosis H37Rv*
Gene names: glf
Method: X-ray diffraction
Resolution: 2.40 Å
Total Structure Weight: 141.52 kDa

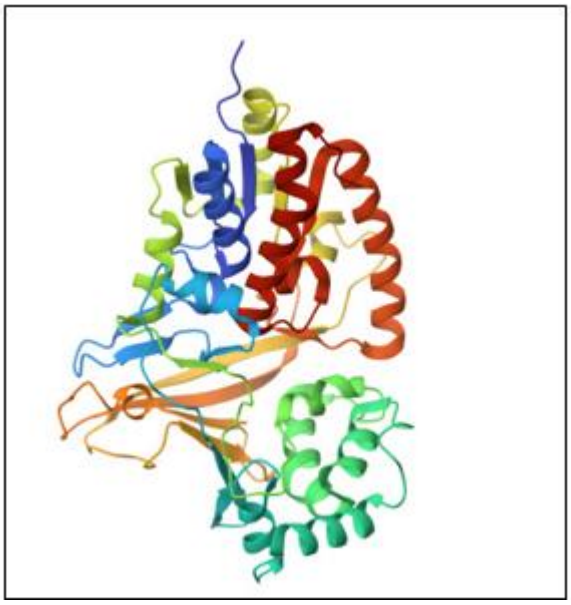

Figure 1: 3D view of UDP-glf (receptor), PDB ID: 4RPG (retrieved from PDB)

A high-quality protein for molecular docking study is shown by the Ramachandran plot, which showed that 91.2% and 8.8% of the amino acid residues lie in the most preferred and additional authorized regions, respectively, and no residues fall in the prohibited regions (Figure 2).

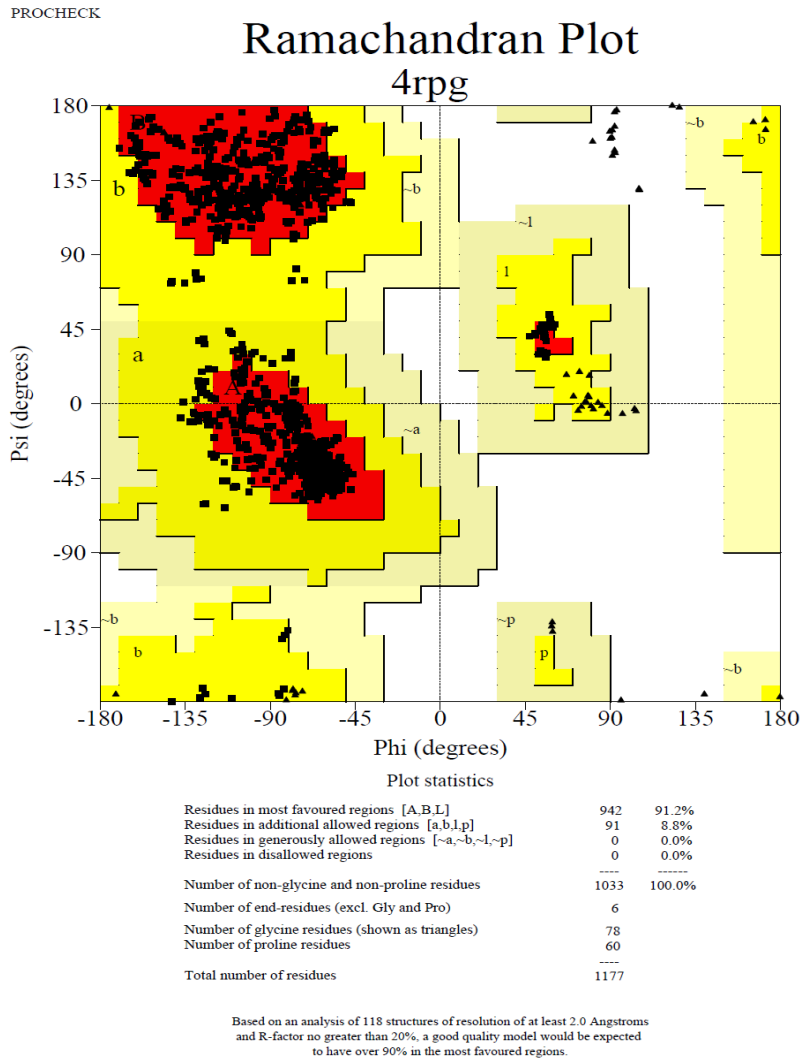

Figure 2: Ramachandran plot showing the statistics of the receptor (using PROCHECK)

Ligands:
Sixteen compounds isolated from *Flacourtia jangomas* plant and the positive control along with their SMILES is given below in Table 1 and their 2D structures are shown in Figure 3.

Sl no.	Compound name	Phytochemical group	SMILES
1	Jangomolide	Limonoid	CC1(C2CC(=O)C3(C(C24C=CC(=O)OC4O1)CCC5(C36C(O6)C(=O)OC5C7=COC=C7)C)C)C
2	Catechin	Flavonols	Oc1ccc(cc1O)C2Oc3cc(O)cc(O)c3CC2O
3	Coumaric acid	Phenolic compound	Oc1ccc(/C=C/C(=O)O)cc1
4	Rutin hydrate	Flavonoid	CC1C(C(C(C(O1)OCC2C(C(C(C(O2)OC3=C(OC4=CC(=CC(=C4C3=O)O)O)C5=CC(=C(C=C5)O)O)O)O)O)O)O)O.O
5	Corymbulosine	Diterpene	CCCCCCCCCC(=O)OC1CC(C(C2C13C(OC(C3=CC(C2)O)OC(=O)C)OC(=O)C)(C)CCC(=C)C=C)C
6	Tremulacin	Salicinoid phenolic glycoside	C1CC(=O)C(C=C1)(C(=O)OCC2=CC=CC=C2OC3C(C(C(C(O3)CO)O)O)OC(=O)C4=CC=CC=C4)O
7	Flacourtin	Phenolic glucoside ester	C1=CC=C(C=C1)C(=O)OCC2C(C(C(C(O2)OC3=CC(=C(C=C3)CO)O)O)O)O
8	Hydnocarpic acid	Cyclopentanoid Fatty acid	C1CC(C=C1)CCCCCCCCCCC(=O)O
9	Chaulmoogric acid	Cyclopentanoid Fatty acid	C1CC(C=C1)CCCCCCCCCCCCC(=O)O
10	Ostruthin	Coumarin	CC(=CCCC(=CCC1=C(C=C2C(=C1)C=CC(=O)O2)O)C)C
11	Ramontoside	Butyrolactone lignin disaccharide	COC1C(COC(C1OC)OC2=C3COC(=O)C3=C(C4=CC(=C(C=C42)OC)OC)C5=CC6=C(C=C5)OCO6)OC7C(C(C(C(O7)CO)O)O)O
12	Beta-sitosterol	Steroid	CCC(CCC(C)C1CCC2C1(CCC3C2CC=C4C3(CCC(C4)O)C)C)C(C)C
13	Beta-D-glucopyranoside	Glucoside	CCCCCCOC1C(C(C(C(O1)CO)O)O)O
14	Quercetin	Flavonoid	C1=CC(=C(C=C1C2=C(C(=O)C3=C(C=C(C=C3O2)O)O)O)O)O
15	Luteolin	Flavonoid	C1=CC(=C(C=C1C2=CC(=O)C3=C(C=C(C=C3O2)O)O)O)O
16	Rutin	Flavonoid	CC1C(C(C(C(O1)OCC2C(C(C(C(O2)OC3=C(OC4=CC(=CC(=C4C3=O)O)O)C5=CC(=C(C=C5)O)O)O)O)O)O)O)O
17	2-aminothiazole (CONTROL)	C1=CSC(=N1)N	

Table 1: Name of sixteen (16) compounds and known inhibitor along with their SMILES

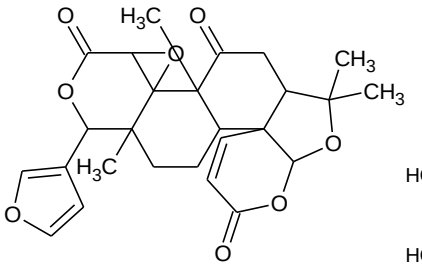

Jangomolide

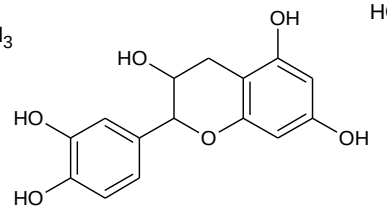

Catechin

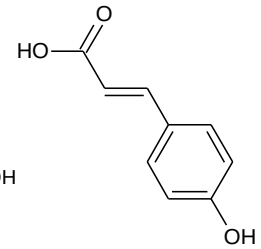

Coumaric acid

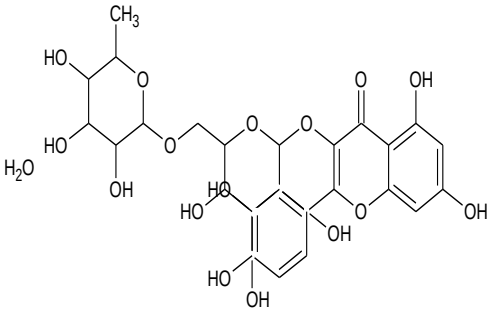

Rutin hydrate

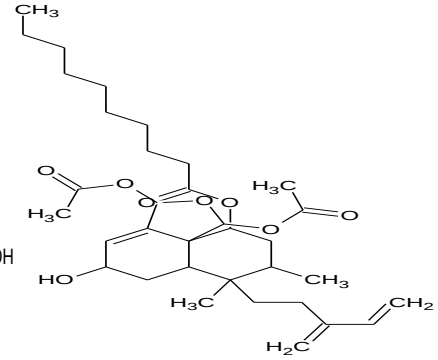

Corymbulosine

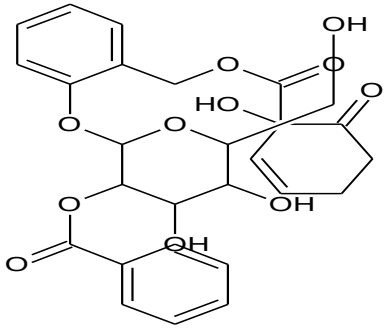

Tremulacin

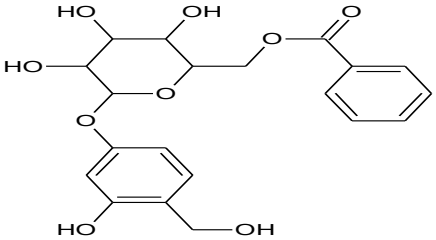

Flacourtin

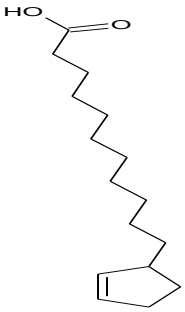

Hydnocarpic acid

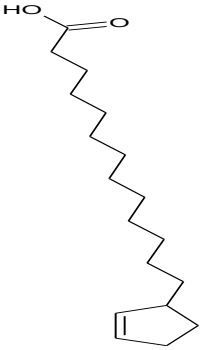

Chaulmoogric acid

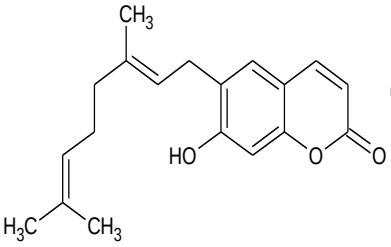

Ostruthin

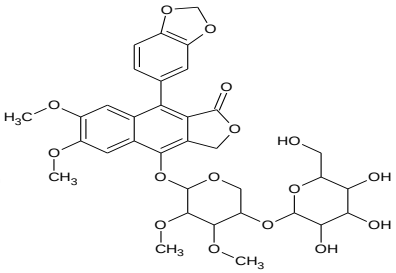

Ramontoside

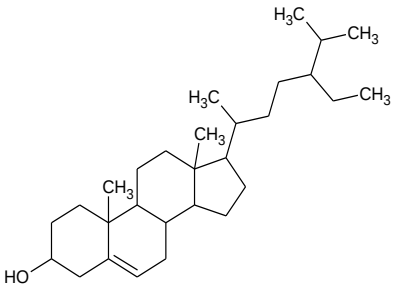

Beta-sitosterol

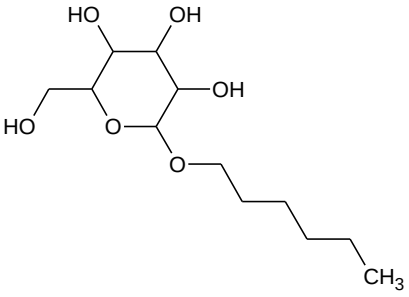

Beta-D- glucopyranoside

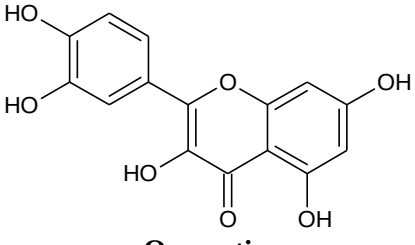

Quercetin

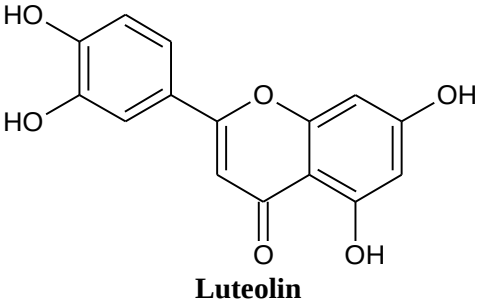

Luteolin

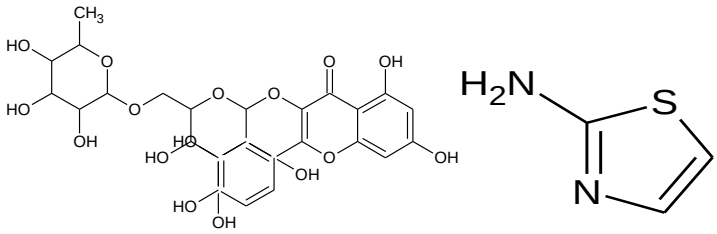

Rutin **2-aminothizole (Control)**

Figure 3: 2D structures of the sixteen phytocompounds of *Flacourtia jangomas* and positive control screened for their binding ability with UDP-glf enzyme.

3.2 Molecular Docking Scores and Inhibition of the receptor:

Based on the molecular docking scores, it was seen that fourteen of the sixteen phytocompounds that were docked against the UDP-glf enzyme had a higher binding affinity with the receptor than the positive control (2-aminothiazole). All these fourteen compounds showed better scores than that of the positive control. Amongst them, two flavonoids namely; Rutin and Quercetin exhibited much stable conformation with UDP-glf having binding energies -33.2935 and -30.8215, k/cal mol^{-1} respectively whereas the control ligand showed a score of -13.3483 k/cal mol^{-1}. A comparative interaction pose of the receptor with the best docked compounds and with the known inhibitor is shown in Figure 4. The total binding energies score of the phytocompounds with their bonded residues are given in Table 2.

Table 2: Binding energy profiles (Kcal/ mol^{-1}) of the sixteen phytocompounds with UDP-glf (4RPG)

Sl no.	Compound	Score	Bonded residues
1	Jangomolide	-16.4382	Tyr305, Arg297
2	Catechin	-30.2623	Pro326, Asp224, Trp225, Arg39, Glu38
3	Coumaric acid	-25.8486	Arg292, Arg180, Met369
4	Rutin hydrate	-33.2940	Arg292, Phe17, Gly44, Ala64, Leu66, Asn46, Tyr62, Arg180
5	Corymbulosine	-3.9846	Arg180, Arg292, Tyr161
6	Tremulacin	-30.2901	Asn282, Tyr161, Arg292, Tyr328, Tyr366, Arg180, Leu66
7	Flacourtin	-26.9150	Tyr161, Arg180, Tyr191, Asp368, His68, Met369
8	Hydnocarpic acid	-14.4960	Tyr305, Arg297
9	Chaulmoorgic acid	-12.9426	Tyr305, Arg297
10	Ostruthin	-16.5801	His68, Arg180, Arg292, Tyr328
11	Ramontoside	-21.5258	Leu66, Arg292, Asn46, Gly362, Thr144, Leu361, Phe18
12	b-sitosterol	-5.9165	Tyr327, Glu325
13	b-D-glucopyranoside	-17.4059	Asn177, Arg180, Tyr161, Arg292, Tyr328
14	Quercetin	-30.8215	Arg249, Arg224, Arg39, Glu38, Trp225, Leu37
15	Luteolin	-27.7081	His89, Arg180, Asn284, Phe157, Asn282
16	Rutin	-33.2935	Arg292, Phe17, Gly44, Ala64, Leu66, Asn46, Tyr52, Arg180
17	2-aminothiazole (control)	-13.3483	Arg297, Asp304, Tyr305

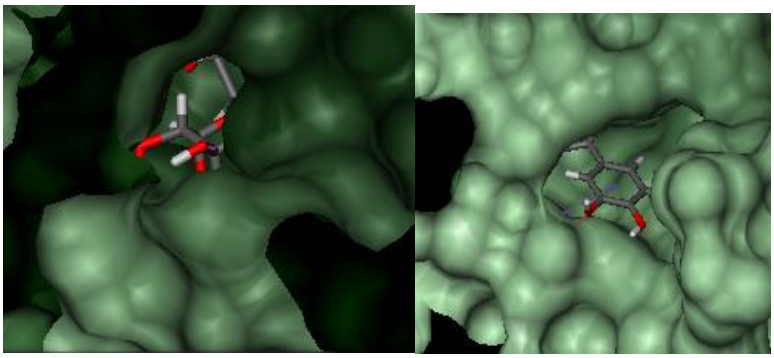

(a) (b)

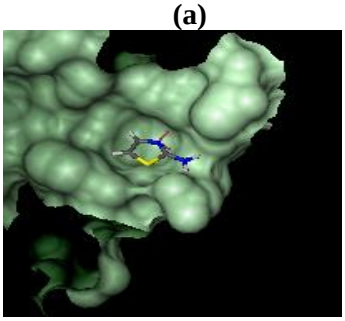

(c)

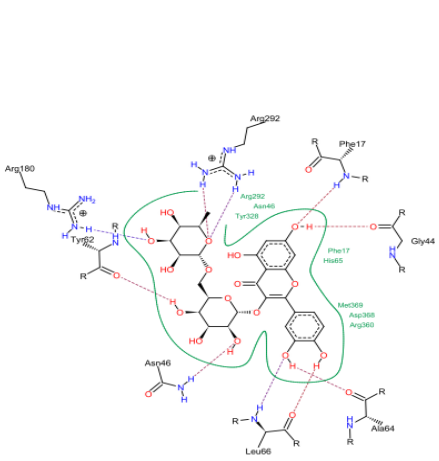

(a)

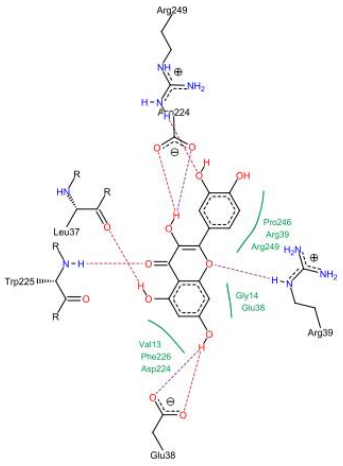

(b)

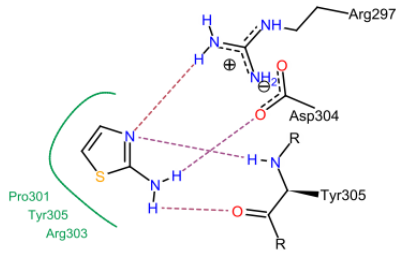

(c)

Figure 4: 3D and 2D docking poses of the compounds which are best docked and the control in the active site of UDP-glf. a: Rutin, b: Quercetin, c. Control (2-aminothiazole)

3.3 QSAR graph:

In the QSAR analysis, the activities of the receptor was correlated with descriptors and the QSAR model was prepared which showed R^2 value is 90.76% (A larger R-squared value suggests a better fit of the equation to the provided data). The adjusted Rsq value is 86.71% which is not of much difference with the main Rsq value (A large disparity between the adjusted and raw R squared suggests a poorer overall forecast). The obtained equation is inefficient if the F statistics value is smaller than the Critical F value, which is 2.44 in

this case. The F statistics value is 22.45. The multiple regression plot for UDP-glf is shown in a graphical pattern in Figure 5.
The generated QSAR equation is:
Activity = -1.552684933115E+000 + 1.816265500233E-003(Mol weight) + -6.680601297057E-003*(Molar volume) + -7.927497686464E-002*(Surface tension) + 2.439909862805E+000*(Density) + 6.370122984671E-001*(LogP) + 3.504200839575E+000*(HBD) + -1.199415035555E-001*(HBA)*

The bioactivities of the recognized inhibitors were estimated using the QSAR equation, compared to the experimental bioactivities, and shown in a scattered plot (Figure 5). It is evident from the plot that the majority of the points lie on or around the trend line, which denotes a decent QSAR equation. From the equation, the bioactivity of compound quercetin was found to be 10.83 which is similar to IC_{50} = 1.47 µM. This value indicated better inhibitory concentration than all the known inhibitors used in QSAR analysis and did not have much difference with the control molecule (Bioactivity=3.36, IC_{50} =0.45 µM).

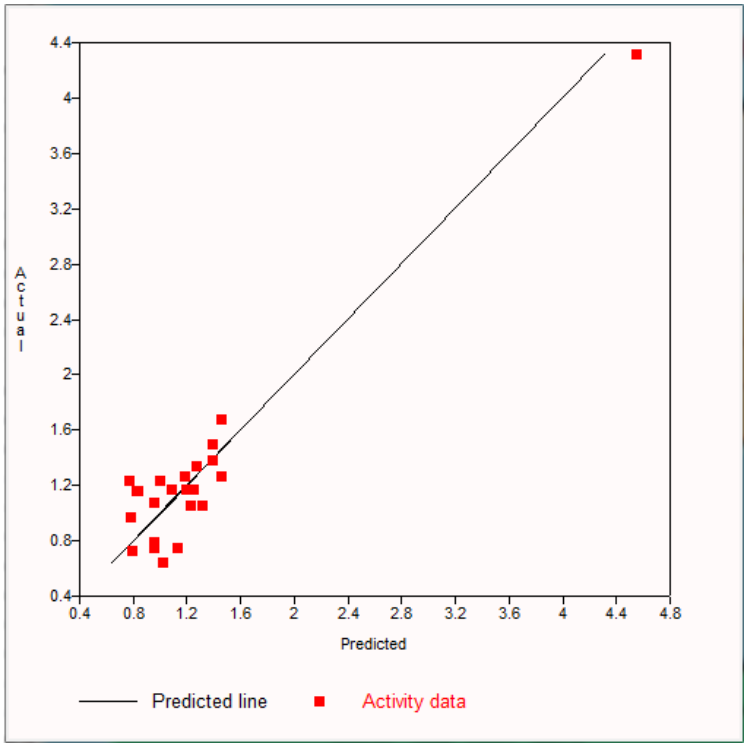

Figure 5:QSAR multiple regression plot showing good correlation.

3.4 ADMET Profile Analysis:

Two compounds namely, Rutin and Quercetin selected after molecular docking were subjected to ADME profiling using SwissADME tool. From the prediction it was observed that only Quercetin showed high Gastro-intestinal (GI) absorption whereas Rutin showed a very low absorption. These results have been reported in Table 3 and BOILED EGG model (Figure 6).In addition Quercetin was shown not to effluate from the Central Nervous System (CNS) by the P-glycoprotein indicating good nature of the compounds as they may not interfere with the CNS.Also quercetin was considered to be substrates of CYP1A2, CYP2D6 and CYP3A4 isoforms of enzymes, which is important in drug elimination through metabolic biotransformation (Diana et al; 2017). Table 3 also displays the pharmokinetics and drug-likeness profile of the two substances, confirming once more that Quercetin exhibit the most encouraging outcomes and do not violate any drug-likeness filters.Quercetin had a moderate of 55% score on the bioavailability scale, indicating a likelihood of at least 10% oral bioavailability in rats or significant Caco-2 permeability (Martin, 2005).An online tool, Molsoft L.L.C was also used to plot a graph to show the drug nature of the compounds (Figure 7)
A web-based tool from Molinspiration Cheminformatics was also used to derive drug-likeness, TPSA, and MiLogP characteristics. By evaluating the activity score of GPCR ligand, ion channel modulator, nuclear receptor ligand, kinase inhibitor, protease inhibitor, and enzyme inhibitor, one can determine the bioactivity of the medication (Kulkarni et al; 2021). According to the bioactivity ratings, quercetin is extremely active (> 0) against enzyme inhibitors, nuclear-receptor ligands, and kinase inhibitors, respectively, whereas rutin is

reported to be very active (> 0) as an enzyme inhibitor. Table 4 displays the modest activity (< 0) of the remaining inhibitors against the two substances.
Toxicity prediction using Protox-II showed the results of many parameters such as oral toxicity class, their predicted LD50 values, tissue and organ toxicity, nuclear receptor signaling pathways and also stresses response pathways. Rutin was considered under GHS Class V chemical compounds (2000<LD50<5000 mg/kg) having LD50 5000 mg/kg respectively while Quercetin was predicted to be under GHS Class III group compounds (50<LD50<300) having LD50 159 mg/kg. The overall toxicity effects of the investigated chemicals on cellular pathways and organ and tissue systems are displayed in Table 5.

Table 3: Calculated pharmacokinetics and drug-likeness parameters of the best two compounds.

Compounds ⟶	Rutin	Quercetin
Pharmacokinetics		
GI absorption	Low	High
BBB permeant	No	No
P-GP substrate	Yes	No
CYP1A2 inhibitor	No	Yes
CYP2C19 inhibitor	No	No
CYP2C9 inhibitor	No	No
CYP2D6 inhibitor	No	Yes
CYP3A4 inhibitor	No	Yes
Dug-likeness rule violation		
Lipinski (Pfizer)	3	0
Ghose (Amgen)	4	0
Veber (GSK)	1	0
Egan (Pharmacia)	1	0
Muegge (Bayer)	4	0
Bioavailability score	0.17	0.55

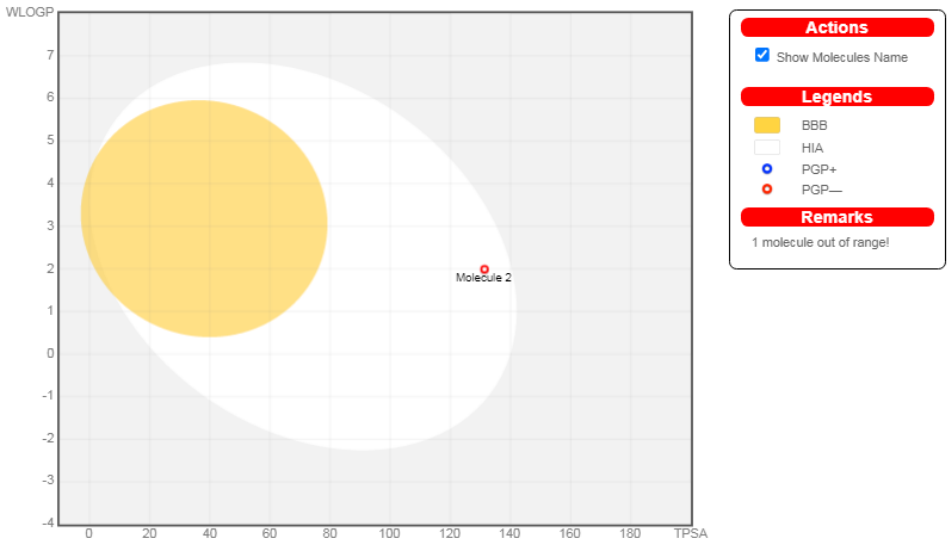

Figure 6: Boiled-Egg Model for Gastrointestinal Absorption and Brain Penetration. It is believed that molecules in the yolk of the egg passively penetrate the blood-brain barrier (BBB), whereas molecules in the white of the egg are passively absorbed by the gastrointestinal tract (GI). Red dots indicate molecules that are not effluated by the P-glycoprotein, while blue dots indicate molecules that are effluated from the Central Nervous System (CNS). Here, molecule 1 (Rutin) is out of range which means it is not absorbed while molecule 2 (Quercetin) is in the white portion of the egg which shows it is well absorbed in the gastrointestinal tract and is also PGP negative.

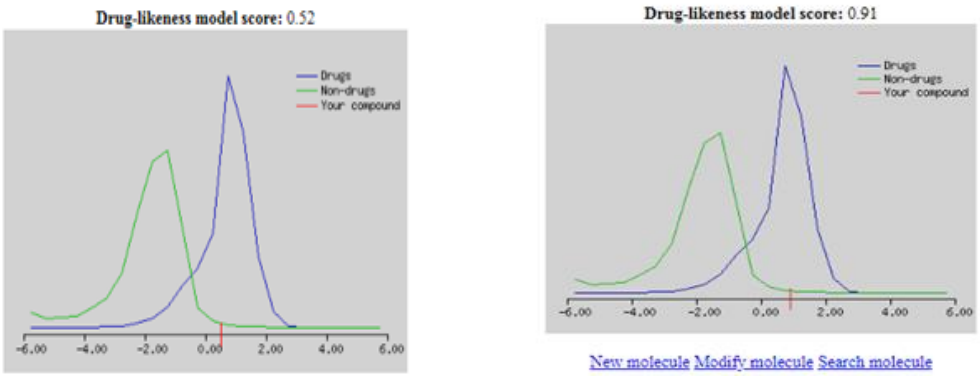

Figure 7: A graph showing drug-likeness score of Quercetin and Rutin

Table 4: Chemical properties and bioactivity score of the best two phytocompounds using Molinspiration tool.

Parameters	Name of the compound	
	Rutin	Quercetin
Chemical Properties		
miLogP	-1.06	1.68
TPSA	269.43	131.35
Natoms	43	22
MW	610.52	302.24
nON	16	7
nOHNH	10	5
Nviolations	3	0
Bioactivity Score		
GPCR ligand	-0.05	-0.06
Ion channel modulator	-0.52	-0.19
Kinase inhibitor	-0.14	0.28
Nuclear receptor ligand	-0.23	0.36
Protease inhibitor	-0.07	-0.25
Enzyme inhibitor	0.12	0.28

Table 5: Toxicity risks parameters on rodent models for high doses of two best compounds (The values in brackets refer to the probability of the prediction)

Compounds	Rutin	Quercetin
Rodent Oral Toxicity		
Predicted LD50 mg/kg	5000	159
Toxicity Class	V	III
Average similarity (%) with training set	100	100
Prediction accuracy (%)	100	100
Tissue and organ toxicity		
Hepatotoxicity	Inactive (0.80)	Inactive (0.69)
Immunotoxicity	Active (0.98)	Inactive (0.87)
Carcinogenecity	Inactive (0.91)	Active (0.68)
Mutagenecity	Inactive (0.88)	Active (0.51)
Cytotoxicity	Inactive (0.64)	Inactive (0.99)
Aryl hydrocarbon Receptor (Ahr)	Inactive (0.83)	Active (0.91)
AR- Androgen Receptor (AR)	Inactive (0.98)	Inactive (0.99)
Androgen Receptor Ligand Binding Domain (AR-LBD)	Inactive (0.99)	Inactive (0.97)
Aromatase (Aro)	Inactive (0.99)	Inactive (0.91)
Estrogen Receptor Alpha (ER)	Inactive (0.95)	Active (0.87)
Estrogen Receptor Ligand Binding Domain (ER-LBD)	Inactive (0.99)	Active (0.95)

PPAR- Gamma- Peroxisome Proliferator Activated Receptor Gamma	Inactive (0.98)	Inactive (0.98)
Nuclear factor {erythroid-derived 2}-like 2/antioxidant responsive element (nfr2/ARE)	Inactive (0.99)	Inactive (0.99)
Heat shock factor response element (HSE)	Inactive (0.99)	Inactive (0.99)
Mitochondrial Membrane Potential (MMP)	Inactive (0.97)	Active (1.0)
Phosphoprotein (tumour suppressor) p53	Inactive (0.90)	Inactive (0.97)
ATPase family AAA domain-containing protein 5 (ATAD5)	Inactive (0.99)	Inactive (0.99)

3.5 Molecular simulation dynamics analysis:

Studies using molecular dynamics and simulation (MD) were conducted to ascertain the 4RPG+Quercetin complex's stability and convergence. A comparison of the root mean square deviation (RMSD) measurements revealed steady conformation during the 100 ns simulation session. The 4RPG protein's Cα-backbone RMSD showed a deviation of 2.5 Å, whereas the ligand quercetin displayed an RMSD of 3 Å (Figure 8A). Every RMSD value falls within the allowed range, which is less than 3 Å. The 4RPG protein linked to the ligand quercetin showed minor variations in its root mean square fluctuations (RMSF) plot; no notable spikes were seen, with the exception of residues 150–155, which may have been caused by the residues' greater flexibility (Figure 8B). The majority of residues exhibit minimal fluctuation throughout the course of the 100 ns simulation (Figure 8B), indicating stable conformations of amino acids during the simulation. Consequently, it may be said from the RMSF plots that, in ligand-bound conformations, the protein structure is stiff during simulation. The compactness of a protein is measured by its radius of gyration, or Rg. The 4RPG Cα-backbone in this investigation showed a steady radius of gyration (Rg) from 14.84 to 14.85 Å when attached to the ligand quercetin (Figure 8C). A ligand-bound protein's very compact orientation is indicated by a significantly stable gyration (Rg). The number of hydrogen bonds forming between the protein and ligand indicates how well the complex interacts and is stable. During the 100 ns simulation period, a substantial four numbers of hydrogen bonds between the enzyme and ligand were observed (Figure 8D). Similar observations were also seen in solvent accessible surface area (SASA) in both the ligand-bound and unbound states, as confirmed by Rg analysis. Figure 8E makes it evident that the protein had a large surface area which was exposed to solvent when the ligand and receptor were not coupled together. When bound with ligand, the SASA value decreased relative to the unbound condition (Figure 8E). The overall analysis of SASA indicates that the binding of ligands causes the corresponding proteins to condense and lose their flexibility.

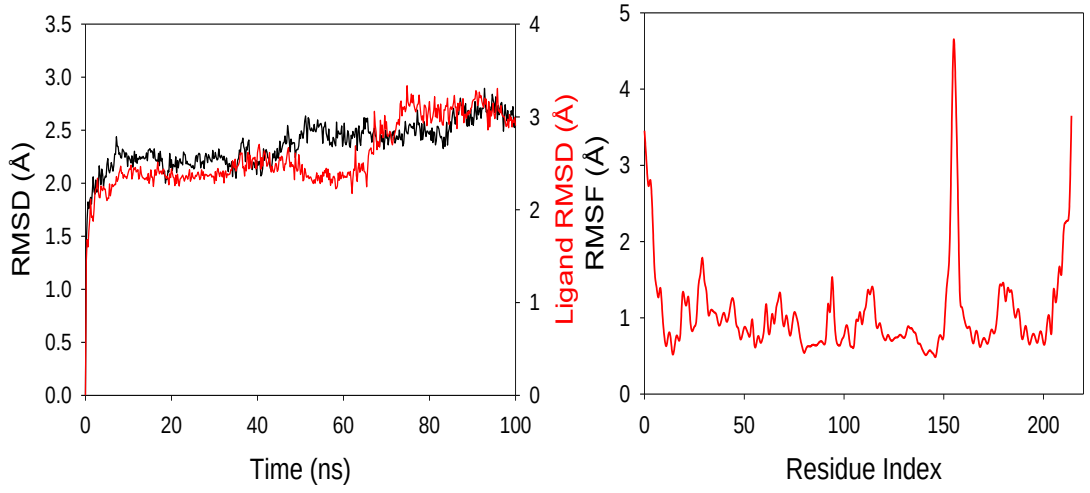

A

B

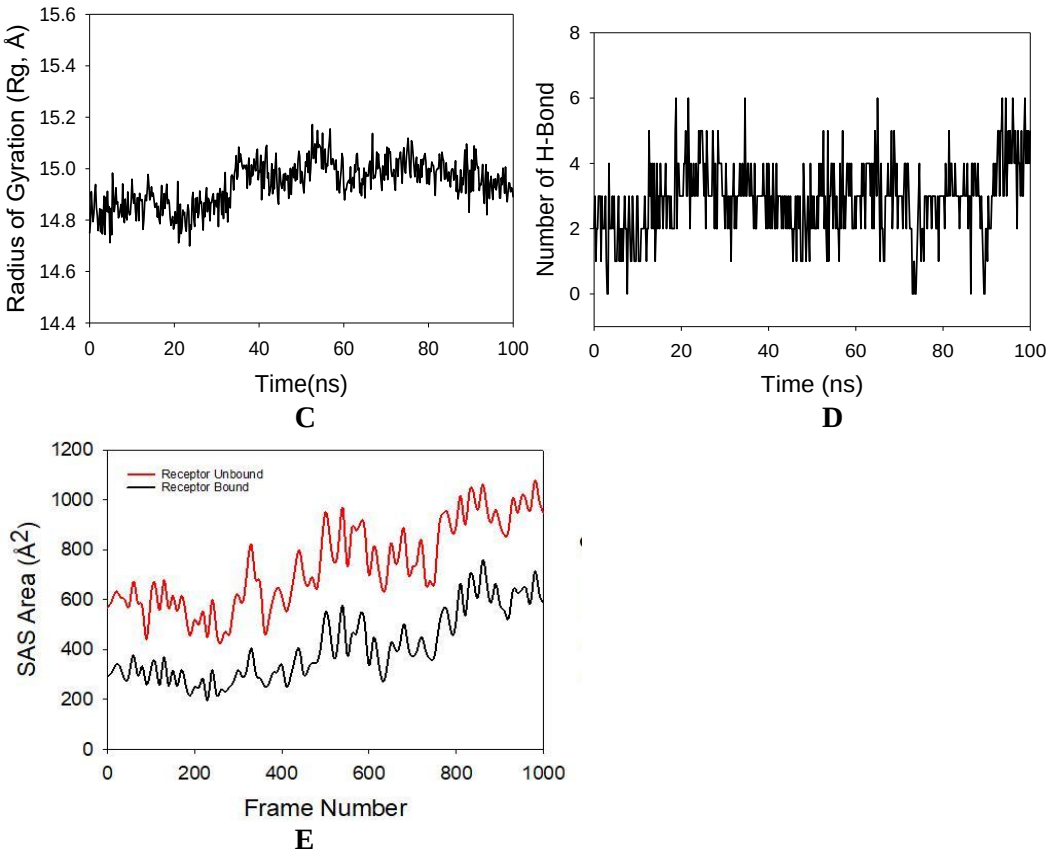

Figure 8: MD simulation analysis of 100 ns trajectories of (A) Cα backbone of 4RPG+Quercetin (B) RMSF of Cα backbone of Lipase bound to Quercetin indicating fluctuating residues with peak around 4.8 Å (C) Radius of gyration (Rg) of Cα backbone of 4RPG+Quercetin (D) Formation of hydrogen bonds in Cα backbone of 4RPG+Quercetin (E) Solvent accessible surface area of Cα backbone of 4RPG+Quercetin where the red peak indicates the ligand unbound state and black peak indicates ligand bound state.

Molecular Mechanics Generalized Born Surface Area (MM-GBSA) calculations

The binding free energy and additional contributing energy in the form of MM-GBSA were found for complex 4RPG+Quercetin using the MD simulation trajectory. The findings (Table 6) indicated that ΔGbindCoulomb, ΔGbindvdW, and ΔGbindLipo contributed the most to ΔGbind in the stability of the simulated complexes, but ΔGbindCovalent and ΔGbindSolvGB contributed to the instability of the corresponding complexes. The binding free energy of the 4RPG+Quercetin complex is noticeably greater (Table 6). These findings provided evidence for the possibility of 4RPG+Quercetin forming stable protein-ligand complexes and for its high affinity and efficiency of binding to the chosen protein.

Table 6. Binding free energy components for the 4RPG+Quercetin calculated from MM-GBSA.

Energies (kcal/mol)	**4RPG+ Quercetin**
ΔG_{bind}	-79.04±2.63
ΔG_{bind}Lipo	-33.96±1.03
ΔG_{bind}vdW	-59.10±2.0
ΔG_{bind}Coulomb	-8.12±1.99
$\Delta G_{bind}H_{bond}$	-0.41±0.22
ΔG_{bind}SolvGB	16.5±1.09
ΔG_{bind}Covalent	1.56±1.2

4. DISCUSSION:

The receptor protein UDP-glf can be considered as an important therapeutic targets in the treatment of tuberculosis due to its importance in the formation of the cell wall in *Mycobacterium tuberculosis*.(Shi et al; 2016, Van et al; 2015). Several studies have indicated that secondary metabolites derived from medicinal plants are effective sources for drug development. Flavonoids, one of the most thoroughly researched

phenolic chemicals, offer a variety of therapeutic characteristics. Many writers have found that flavonoids have a good effect on tuberculosis as an anti-tubercular medication. (Rabaan et al; 2022, Kumar et al; 2021, Yadav et al; 2022, Maiolini et al; 2020). The herb *Flacourtia jangomas* hasn't been utilised very frequently, and there aren't many reports of its anti-tubercular activity. So, using computational analysis, the present work has examined the significance of the *Flacourtia jangomas* plant as an anti-tubercular medicine.

According to our current research, a significant percentage of the sixteen (16) phytochemicals extracted from the *Flacourtia jangomas* plant (reported by Sasi et al.) performed better in molecular docking tests than the control molecule. With scores of-33.2953 kcal/mol and -30.8215 kcal/molrespectively, rutin and quercetin had the greatest binding affinity with the target receptor UDP-glf. These docking data can be compared to the Swain et al. study from 2021, which found that among seven polyphenol compounds, quercetin had the highest binding score to isoniazid. Again, comparable results that confirmed the therapeutic potential of quercetin were found in the investigations conducted by Hasan et al. in 2022 and Rabban et al in the same year.

The inverse logarithm of the IC50 has been used by the QSAR model to forecast the activity of the questioned molecule (Patani G.A. 1996). The compounds that demonstrated the best docking scores against this target when compared to others were used to generate the QSAR equation and plot the multiple regression graph for UDP-glf.

Although the potential of these compounds has been determined by their binding scores, any compound that is to become a therapeutic molecule must be non-toxic, free of other negative effects, and have all ADME qualities (Laskar M.A et al; 2014). Swiss ADME, Molsinspiration, Molsoft, and the Protox-II web application were used for ADME/Tox profiling. The pharmaceutical industry usually accepts these *in silico* toxicological analysis methodologies for usage in making decisions during the medicine development procedures for validation (Dahlgren and Lennernas; 2019, Laskar YB etal, 2021.). The boiled egg model also suggested that quercetin would be passively absorbed by the gastro-intestinal tract as it met all five druglikeliness rules (Lipinski, Ghose, Veber, Egan, Muegge) according to the toxicological results. Quercetin's TPSA score of 131.35 verified its status as a reliable indicator of intestinal absorption. These findings can be compared to those of Md. Mahmudul Hasan and his colleagues' studies from 2022, which examined the ADME/T characteristics of quercetin against a variety of illnesses, tuberculosis being one of them. Another study (Ouahab Ammar; 2017) found quercetin to have a similar effect. The polyherbal mixture of rutin, quercetin, and curcumin did not cause any toxicity in mice and should be highly beneficial for any further *in vivo* and clinical research. According to Tiwari R et al.'s 2020 assessment, this combination is safe.

Additionally, Quercetin upto a range of 5000 mg/kg is non-toxic and is safe to use up to 2000 mg/kg, according to Tiwari et al. Quercetin was classified under Class III toxicity with 100% prediction accuracy according to the toxicity classes given by Drwal et al (2014). On the other hand, quercetin does not have negative health consequences when consumed at amounts consistent with dietary intake. Quercetin was found to be ineffective against hepatotoxicity, immunotoxicity, and cytotoxicity in the toxicity endpoint assays. The findings of Gelen V et al (2017) and M M Hasan et al (2022) supported that quercetin has protective benefits against 5-FU-induced hepatotoxicity and is safe to use because it shows no mutagenic or carcinogenic qualities.

Also, quercetin had beneficial outcomes for a number of parameters in the Tox-21 stress response and nuclear receptor signaling pathways. In a study akin to this one, Bardbori A. M. (2012) found quercetin to indirectly activate Ahr. The results of Woude H.V et al (2006), Wilkinson A.S et al (2005), and Shahzad H et al (2014) offer supporting evidence for ER and ER-LBD pathways. Quercetin displayed an active status for mitochondrial membrane potential while in the stress response pathway. Quercetin was also discovered to influence a number of pathways connected to mitochondria, including those for mitochondrial biogenesis, MMP, oxidative respiration, and many others (Marcos Roberto de Oliveira et al., 2016).According to a study published in 2021 by Vissenaekens H et al; 2021, quercetin can partially reverse mitochondrial dysfunction brought on by FCCP. This effect was correlated with an accumulation of intracellular quercetin in the mitochondria of intestinal cells.

Finally, a molecular dynamics simulation lasting 100 ns was carried out to assess the stability and quality of the best docked protein-ligand. These findings demonstrated stable conformations with acceptable RMSD and RMSF values. In a simulation process, the stability of RMSD plots indicates better convergence and stable conformations throughout the simulation (Ahmad I et al; 2023; Aier I et al; 2016; Castrosanto M A et al; 2022). Thus, it can be concluded that when 4RPG binds to quercetin, it creates a fairly stable complex. In a similar vein, little fluctuation spikes were visible in the RMSF graphs, suggesting steady conformation

through the entire simulation period. Furthermore, the radius of gyration (Rg) of the protein-ligand complex showed nearly consistent values. The protein complex is more compact when it is attached to the ligand, as indicated by the lower and steadier Rg peak. Furthermore, the significance of the interaction and the stability of the complex are indicated by the quantity of H-bonds that forms between a protein and a ligand (Ahmad I et al; 2023).Proteins' solvent accessible surface area (SASA) has long been regarded as a key component in investigations into protein folding and stability. It is described as the surface surrounding a protein that has the molecule's van der Waals contact surface and a hypothetical solvent sphere center (Ali S A et al; 2023). The SASA values point to a potential strong protein-ligand interaction in the biological environment. As a result, it can be inferred that the complexes to which quercetin is attached are quite stable since the ligand has a stronger affinity and allows to predict quercetin as a potent inhibitor of UDP-glf during tuberculosis protection.

5. CONCLUSION:

Given the huge need for anti-tuberculosis medications, it can be inferred from the aforementioned *in silico* research that natural phytochemicals may assist in the process of drug discovery. The study's conclusive results all point to the possibility that quercetin, a flavonoid isolated from *Flacourtia jangomas*, in relation to *Mtb* UDP-glf could shed light on its potential utility in tuberculosis control after more standardized *in vitro* and *in vivo* validation in the future. This outcome might aid in the creation of a new anti-tuberculosis treatment lead.

6. ACKNOWLEDGEMENT:

The Bioinformatics and Computational Biology Centre at Assam University in Silchar provided the lab space needed for the experiment, for which the authors are thankful. The literature search tools provided by DeLCON are highly appreciated by the authors.

7. CONFLICT OF INTEREST:

The authors report no conflict of interest arising out of this article. The work does not involve human or animals for its experiments hence ethical constrain does not arise.

8. REFERENCES:

1. Abrahams, K.A., Besra, G.S., 2018. Mycobacterial cell wall biosynthesis: a multifaceted antibiotic target. Parasitology 145, 116-133.
2. Adeniji, S.E., Uba, S., Uzairu, A., 2018. QSAR modeling and molecular docking analysis of some active compounds against mycobacterium tuberculosis receptor (Mtb CYP121). Journal of pathogens 2018.
3. Ahmad, I., Hoque, M., Alam, S.S.M., Zughaibi, T.A., Tabrez, S., 2023. Curcumin and Plumbagin Synergistically Target the PI3K/Akt/mTOR Pathway: A Prospective Role in Cancer Treatment. International Journal of Molecular Sciences 24, 6651.
4. Aier, I., Varadwaj, P.K., Raj, U., 2016. Structural insights into conformational stability of both wild-type and mutant EZH2 receptor. Scientific reports 6, 34984.
5. Alderwick, L.J., Harrison, J., Lloyd, G.S., Birch, H.L., 2015. The mycobacterial cell wall—peptidoglycan and arabinogalactan. Cold Spring Harbor perspectives in medicine 5, a021113.
6. Ali, A., Wani, A.B., Malla, B.A., Poyya, J., Dar, N.J., Ali, F., Ahmad, S.B., Rehman, M.U., Nadeem, A., 2023. Network Pharmacology Integrated Molecular Docking and Dynamics to Elucidate Saffron Compounds Targeting Human COX-2 Protein. Medicina 59, 2058.
7. Amado, P.S., Woodley, C., Cristiano, M.L., O'Neill, P.M., 2022. Recent advances of DprE1 inhibitors against mycobacterium tuberculosis: computational analysis of physicochemical and ADMET properties. ACS omega 7, 40659-40681.
8. Ammar, O., 2017. In silico pharmacodynamics, toxicity profile and biological activities of the Saharan medicinal plant Limoniastrum feei. Brazilian Journal of Pharmaceutical Sciences 53.
9. Atanasov, A.G., Zotchev, S.B., Dirsch, V.M., Supuran, C.T., 2021. Natural products in drug discovery: Advances and opportunities. Nature reviews Drug discovery 20, 200-216.

10. Banerjee, P., Eckert, A.O., Schrey, A.K., Preissner, R., 2018. ProTox-II: a webserver for the prediction of toxicity of chemicals. Nucleic acids research 46, W257-W263.
11. Bowers, K.J., Chow, E., Xu, H., Dror, R.O., Eastwood, M.P., Gregersen, B.A., Klepeis, J.L., Kolossvary, I., Moraes, M.A., Sacerdoti, F.D., 2006. Scalable algorithms for molecular dynamics simulations on commodity clusters, Proceedings of the 2006 ACM/IEEE Conference on Supercomputing, pp. 84-es.
12. Castrosanto, M.A., Mukerjee, N., Ramos, A.R., Maitra, S., Manuben, J.J.P., Das, P., Malik, S., Hasan, M.M., Alexiou, A., Dey, A., 2022. Abetting host immune response by inhibiting rhipicephalus sanguineus Evasin-1: An in silico approach. Plos one 17, e0271401.
13. Chawla, R., Rani, V., Mishra, M., 2022. Changing paradigms in the treatment of tuberculosis. Indian Journal of Tuberculosis 69, 389-403.
14. Chow, E., Rendleman, C.A., Bowers, K.J., Dror, R.O., Hughes, D.H., Gullingsrud, J., Sacerdoti, F.D., Shaw, D.E., 2008. Desmond performance on a cluster of multicore processors. DE Shaw Research Technical Report DESRES/TR--2008-01.
15. Cobelens, F., Suri, R.K., Helinski, M., Makanga, M., Weinberg, A.L., Schaffmeister, B., Deege, F., Hatherill, M., 2022. Accelerating research and development of new vaccines against tuberculosis: a global roadmap. The Lancet Infectious Diseases.
16. Dahlgren, D., Lennernäs, H., 2019. Intestinal permeability and drug absorption: predictive experimental, computational and in vivo approaches. Pharmaceutics 11, 411.
17. Daina, A., Michielin, O., Zoete, V., 2017. SwissADME: a free web tool to evaluate pharmacokinetics, drug-likeness and medicinal chemistry friendliness of small molecules. Scientific reports 7, 42717.
18. Daina, A., Zoete, V., 2016. A boiled-egg to predict gastrointestinal absorption and brain penetration of small molecules. ChemMedChem 11, 1117-1121.
19. de Oliveira, M.R., Nabavi, S.M., Braidy, N., Setzer, W.N., Ahmed, T., Nabavi, S.F., 2016. Quercetin and the mitochondria: a mechanistic view. Biotechnology advances 34, 532-549.
20. Dean, A.S., Auguet, O.T., Glaziou, P., Zignol, M., Ismail, N., Kasaeva, T., Floyd, K., 2022. 25 years of surveillance of drug-resistant tuberculosis: achievements, challenges, and way forward. The Lancet Infectious Diseases 22, e191-e196.
21. Drwal, M.N., Banerjee, P., Dunkel, M., Wettig, M.R., Preissner, R., 2014. ProTox: a web server for the in silico prediction of rodent oral toxicity. Nucleic acids research 42, W53-W58.
22. Gelen, V., Şengül, E., Gedikli, S., Atila, G., Uslu, H., Makav, M., 2017. The protective effect of rutin and quercetin on 5-FU-induced hepatotoxicity in rats. Asian Pacific Journal of Tropical Biomedicine 7, 647-653.
23. George, S.A., Bhadran, S., Sudhakar, M., BP, H., 2017. Comprehensive in Vitro Evaluation of Pharmacological Activities of Selected Plant Extracts and Gas Chromatograph Y-Mass Spectrometry Profiling of Flacourtia Jangomas Flower Extract. Asian Journal of Pharmaceutical and Clinical Research 10, 237.
24. Hasan, M.M., Khan, Z., Chowdhury, M.S., Khan, M.A., Moni, M.A., Rahman, M.H., 2022. In silico molecular docking and ADME/T analysis of Quercetin compound with its evaluation of broad-spectrum therapeutic potential against particular diseases. Informatics in Medicine Unlocked 29, 100894.
25. Jorgensen, W.L., Chandrasekhar, J., Madura, J.D., Impey, R.W., Klein, M.L., 1983. Comparison of simple potential functions for simulating liquid water. The Journal of chemical physics 79, 926-935.
26. K Mishra, R., Singh, J., 2015. A structure guided QSAR: a rapid and accurate technique to predict IC50: a case study. Current Computer-Aided Drug Design 11, 152-163.
27. Kashyap, S., Srivastava, A., Saxena, P.S., 2017. Biosynthesis of silver nanoparticles from Flacortia jangomas leaf extract and its bactericidal application against E. coli. Int J Mater Sci 12, 104-107.
28. Kulkarni, P., Walunj, Y., Dongare, N., 2021. Theoretical Validation of Medicinal Properties of Ocimum sanctum. The Chemist, 53.
29. Kumar, M., Singh, S.K., Singh, P.P., Singh, V.K., Rai, A.C., Srivastava, A.K., Shukla, L., Kesawat, M.S., Kumar Jaiswal, A., Chung, S.-M., 2021. Potential anti-Mycobacterium tuberculosis activity of plant secondary metabolites: insight with molecular docking interactions. Antioxidants 10, 1990.
30. Laskar, M.A., Choudhury, M.D., 2014. Journal of Drug Discovery and Therapeutics 2 (23) 2014, 24-31. Journal of Drug Discovery and Therapeutics 2, 24-31.
31. Laskar, Y.B., Mazumder, P.B., Talukdar, A.D., 2023. Hibiscus sabdariffa anthocyanins are potential modulators of estrogen receptor alpha activity with favourable toxicology: a computational analysis using molecular docking, ADME/Tox prediction, 2D/3D QSAR and molecular dynamics simulation. Journal of Biomolecular Structure and Dynamics 41, 611-633.

32. Liebenberg, D., Gordhan, B.G., Kana, B.D., 2022. Drug resistant tuberculosis: Implications for transmission, diagnosis, and disease management. Frontiers in Cellular and Infection Microbiology, 1443.
33. Maiolini, M., Gause, S., Taylor, J., Steakin, T., Shipp, G., Lamichhane, P., Deshmukh, B., Shinde, V., Bishayee, A., Deshmukh, R.R., 2020. The war against tuberculosis: a review of natural compounds and their derivatives. Molecules 25, 3011.
34. Maitra, A., Munshi, T., Healy, J., Martin, L.T., Vollmer, W., Keep, N.H., Bhakta, S., 2019. Cell wall peptidoglycan in Mycobacterium tuberculosis: An Achilles' heel for the TB-causing pathogen. FEMS Microbiology Reviews 43, 548-575.
35. Martin, Y.C., 2005. A bioavailability score. Journal of medicinal chemistry 48, 3164-3170.
36. Martyna, G.J., Klein, M.L., Tuckerman, M., 1992. Nosé–Hoover chains: The canonical ensemble via continuous dynamics. The Journal of chemical physics 97, 2635-2643.
37. Martyna, G.J., Tobias, D.J., Klein, M.L., 1994. Constant pressure molecular dynamics algorithms. The Journal of chemical physics 101, 4177-4189.
38. Mishra, T., Rai, A., 2020. A critical review of Flacourtia Jangomas (Lour) Raeusch: A Rare Fruit Tree of Gorakhpur Division.
39. Mohammadi-Bardbori, A., Bengtsson, J., Rannug, U., Rannug, A., Wincent, E., 2012. Quercetin, resveratrol, and curcumin are indirect activators of the aryl hydrocarbon receptor (AHR). Chemical research in toxicology 25, 1878-1884.
40. Mohan, A.C., Geetha, S., Gajalakshmi, R., Divya, S., Dhanarajan, M., 2017. Determination of molecular property, bioactivity score and binding energy of the phytochemical compounds present in Cassia auriculata by molinspiration and DFT method. Texila International Journal of Basic Medical Science 2, 1-15.
41. Pai, A., Shenoy, K., 2021. Physicochemical and phytochemical analysis of methanolic extract of leaves and fruits of Flacourtia jangomas (Lour.) Raeusch. International Journal of Pharmaceutical Sciences and Research 12, 1671-1678.
42. Patani, G.A., LaVoie, E.J., 1996. Bioisosterism: a rational approach in drug design. Chemical reviews 96, 3147-3176.
43. Rabaan, A.A., Alhumaid, S., Albayat, H., Alsaeed, M., Alofi, F.S., Al-Howaidi, M.H., Turkistani, S.A., Alhajri, S.M., Alahmed, H.E., Alzahrani, A.B., 2022. Promising antimycobacterial activities of flavonoids against Mycobacterium sp. drug targets: A comprehensive review. Molecules 27, 5335.
44. Rarey, M., Kramer, B., Lengauer, T., Klebe, G., 1996. A fast flexible docking method using an incremental construction algorithm. Journal of molecular biology 261, 470-489.
45. Rosell-Hidalgo, A., Young, L., Moore, A.L., Ghafourian, T., 2021. QSAR and molecular docking for the search of AOX inhibitors: a rational drug discovery approach. Journal of Computer-Aided Molecular Design 35, 245-260.
46. Saikia, S., Mahnot, N.K., Mahanta, C.L., 2016. Phytochemical content and antioxidant activities of thirteen fruits of Assam, India. Food bioscience 13, 15-20.
47. Sasi, S., Anjum, N., Tripathi, Y., 2018. Ethnomedicinal, phytochemical and pharmacological aspects of Flacourtia jangomas: a review. International Journal of Pharmacy and Pharmaceutical Sciences, 9-15.
48. Shahzad, H., Giribabu, N., Muniandy, S., Salleh, N., 2014. Quercetin induces morphological and proliferative changes of rat's uteri under estrogen and progesterone influences. International journal of clinical and experimental pathology 7, 5484.
49. Shi, Y., Colombo, C., Kuttiyatveetil, J.R., Zalatar, N., van Straaten, K.E., Mohan, S., Sanders, D.A., Pinto, B.M., 2016. A Second, Druggable Binding Site in UDP-Galactopyranose Mutase from Mycobacterium tuberculosis? ChemBioChem 17, 2264-2273.
50. Shivakumar, D., Williams, J., Wu, Y., Damm, W., Shelley, J., Sherman, W., 2010. Prediction of absolute solvation free energies using molecular dynamics free energy perturbation and the OPLS force field. Journal of chemical theory and computation 6, 1509-1519.
51. Shukla, S., Naik, G., Mishra, S.K., 2015. Potential antimicrobial activity of bacterial endophytes isolated from Flacourtia jangomas (Lour.) Raeusch, a less explored medicinal plant. The Journal of Microbiology, Biotechnology and Food Sciences 4, 473.
52. Soltero-Higgin, M., Carlson, E.E., Gruber, T.D., Kiessling, L.L., 2004. A unique catalytic mechanism
53. Swain, S.S., Pati, S., Hussain, T., 2022. Quinoline heterocyclic containing plant and marine candidates against drug-resistant Mycobacterium tuberculosis: A systematic drug-ability investigation. European Journal of Medicinal Chemistry 232, 114173.

54. Swain, S.S., Rout, S.S., Sahoo, A., Oyedemi, S.O., Hussain, T., 2021. Antituberculosis, antioxidant and cytotoxicity profiles of quercetin: a systematic and cost-effective in silico and in vitro approach. Natural Product Research 36, 4757-4761.
55. Tiwari, R., Siddiqui, M.H., Mahmood, T., Farooqui, A., Bagga, P., Ahsan, F., Shamim, A., 2020. An exploratory analysis on the toxicity & safety profile of Polyherbal combination of curcumin, quercetin and rutin. Clinical Phytoscience 6, 1-18.
56. Toukmaji, A.Y., Board Jr, J.A., 1996. Ewald summation techniques in perspective: a survey. Computer physics communications 95, 73-92.
57. van der Woude, H., 2006. Mechanisms of toxic action of the flavonoid quercetin and its phase II metabolites. Ponsen & Looijen.
58. Van Straaten, K.E., Kuttiyatveetil, J.R., Sevrain, C.M., Villaume, S.A., Jimenez-Barbero, J., Linclau, B., Vincent, S.P., Sanders, D.A., 2015. Structural basis of ligand binding to UDP-galactopyranose mutase from Mycobacterium tuberculosis using substrate and tetrafluorinated substrate analogues. Journal of the American chemical society 137, 1230-1244.
59. Vissenaekens, H., Smagghe, G., Criel, H., Grootaert, C., Raes, K., Rajkovic, A., Goeminne, G., Boon, N., De Schutter, K., Van Camp, J., 2021. Intracellular quercetin accumulation and its impact on mitochondrial dysfunction in intestinal Caco-2 cells. Food Research International 145, 110430.
60. Weston, A., Stern, R., Lee, R., Nassau, P., Monsey, D., Martin, S., Scherman, M., Besra, G., Duncan, K., McNeil, M., 1998. Biosynthetic origin of mycobacterial cell wall galactofuranosyl residues. Tubercle and Lung Disease 78, 123-131.
61. Wilkinson, A.S., Taing, M.-W., Pierson, J.T., Lin, C.-N., Dietzgen, R.G., Shaw, P.N., Gidley, M.J., Monteith, G.R., Roberts-Thomson, S.J., 2015. Estrogen modulation properties of mangiferin and quercetin and the mangiferin metabolite norathyriol. Food & function 6, 1847-1854.
62. Winkler, D.A., 2002. The role of quantitative structure-activity relationships (QSAR) in biomolecular discovery. Briefings in bioinformatics 3, 73-86.
63. Yadav, M., Sharma, P., 2022. Plant-derived Molecules for the Treatment of Tuberculosis: A Review. Iraqi Journal of Pharmaceutical Sciences (P-ISSN 1683-3597 E-ISSN 2521-3512) 31, 1-13.
64. Global TB Report, WHO, 2022, 2023.